Geology of Ore Deposits, Vol. 45, No. 5, 2003, pp. 375–394. Translated from Geologiya Rudnykh Mestorozhdenii, Vol. 45, No. 5, 2003, pp. 429–451.

The Maisk Quartz Gold Deposit (Northern Karelia): Geological, Mineralogical, and Geochemical Studies and Some Genetic Problems

Yu. G. Safonov, A. V. Volkov[1], A. A. Wolfson, A. D. Genkin, T. L. Krylova, and A. V. Chugaev

Institute of Geology of Ore Deposits, Petrography, Mineralogy, and Geochemistry, Russian Academy of Sciences (IGEM RAS), Staromonetnyi per. 35, Moscow, 119017 Russia

Received May 27, 2003

Abstract—The paper contains results of geological, structural, mineralogical, isotopic, and thermobarogeochemical studies of one of the few known gold deposits in the Early Proterozoic greenstone belt of North Karelia. The Maisk deposit is localized in the Kuolajarvi structure, 80% of which is occupied by volcanic and intrusive basic and ultrabasic rocks. The shape of orebodies at the deposit is related to the deformations within the ore-bearing faults. The formation of veins at the deposit was accompanied by rock disintegration and its replacement by quartz. Three stages of mineral formation are distinguished: (1) formation of quartz bodies; (2) deposition of the gold–sulfide assemblage in the quartz bodies synchronously with the biotite + albite + amphibole + chlorite metasomatic rocks; and (3) deposition of the quartz + carbonate + chlorite + talc assemblage. The deposition of the vein quartz began at 470–300°C. The ore fluid was heterogenic, saturated with gas of low density, and of low fluid pressure. Sulfides were deposited at a temperature of around 200°C from fluid with 22–26 wt % salinity. The main salt in the solution was $CaCl_2$, and the methane content varied from 16–25 to 70–100 mol %. Pressure and temperature decreased during the sulfide deposition from 940 to 500 bar and from 270 to 190°C, respectively. The gold was deposited at 200–140°C from solution with 22–28 wt % salinity and with $CaCl_2$ as the predominant salt. According to the stable isotope (^{18}O, ^{13}C, and ^{34}S) data, the hydrothermal fluids that formed the quartz veins and ore mineralization were composed mainly of magmatic water. The isotope composition of Pb corresponds to the crustal source of the ore metals. The K–Ar age data of metasomatic and vein minerals fall into two groups: 1800–1700 and 1610 ± 30 Ma.

INTRODUCTION

The Maisk deposit in northeast Karelia was discovered in 1971. This is the only occurrence of poor sulfide quartz gold mineralization in the Karelia–Kola region. It is rather well explored and studied today. Though the deposit is small, it is important for the region, because there are a lot of quartz veins there and the gold-bearing quartz is abundant in glacial moraines. The quartz gold vein deposits have not yet been discovered in the neighboring Finnish territory. Only veinlet–disseminated, vein, gold–sulfide, and gold-bearing massive sulfide deposits are known there.

The Maisk deposit was studied by geologists of the Central Kola Prospecting Enterprise (A.D. Dain, V.I. Bezrukov, and some others), TsNIGRI (the Central Scientific Geological Prospecting Institute), the Geological Institute of the Kola Research Center of the Russian Academy of Sciences, and others. Authors of this paper studied the deposit in 1974 and 1984 (Yu.G. Safonov, with M.I. Sidyakin and A.K. Kulnev) and then in 1998 and 1999 (A.V. Volkov and A.A. Wolfson) after the incomplete mining of the deposit. Safonov and Volkov visited some gold deposits in northern Finland in 2002. All collected data, including analytical results of the prospecting enterprise, served as the basis for this paper.

[1]Corresponding author: A. Volkov. E-mail: alexandr@igem.ru

GEOLOGICAL SETTING

The Maisk deposit occurs in the central part of the Lapland or Lapland–Karelian greenstone belt. The belt is composed of Early Proterozoic metamorphosed terrigenous and basic volcanic rocks (Fig. 1). Intrusive rocks are granites, gabbrodiabases, peridotites, and pyroxenites (Ward *et al.*, 1989).

The geodynamical evolution of the Lapland–Karelian belt (as that of the whole Baltic shield) has various interpretations. The Maisk deposit occurs in the Salla–Pana–Kuolajarvi zone, consisting of two subzones: the meridional Salla–Kuolajarvi subzone and the latitudinal Kuusamo–Paanajarvi subzone. The deposit occurs in the eastern part of the first subzone in the immediate vicinity of its conjugation with the Kuusamo–Paanajarvi subzone (Fig. 2). The morphology of the Kuolajarvi graben–syncline is defined by large deep-rooted faults that were inherited from a riftogenic depression of the Karelian tectonomagmatic stage (Mitrofanov *et al.*, 1995). The strike of the regional faults varies within the Kuolajarvi structure from NW to NE to the south of the deposit, where they conjugate with latitu-

Fig. 1. Distribution of the gold deposits in the Lapland greenstone belt (based on data of Pankka and Vanhanen (1989), with additions). Gold deposits: (**1**) Bidjovazh; (**2**) Juomasuo; (**3**) Maisk; (**4**) Suriikusiko; (**5**) Pahtavaara; (**6**) Saattapora.

inal faults (Fig. 2). An important tectonic feature is tting of the deposit at the conjugation of the Belo-iorsk–Karelian megablock with the South–Lapland ne (Voinov and Polekhovskii, 1985; Mints *et al.*, 996).

The Kuolajarvi structure is a cuplike depression 00 × 300 km, elongated in the NW direction (Fig. 2). he main part of the depression is situated in Finnish erritory, and only its eastern limb occurs in Russia. his limb dips to the west as a monocline under a vary-ng angle (Fig. 3). The basic volcanics predominant (up o 80%) in the Kuolajarvi structure alternate with vari-us sedimentary rocks (Malezhik *et al.*, 1983). The nterlayer bodies and sills of intrusive or subvolcanic netagabbros, metapyroxenites, and metaperidotites are omagmatic with volcanic rocks and have similar hemical compositions. The rocks are metamorphosed n epidote–amphibolite facies in the eastern margin of he structure and in the greenschist facies in its central part. The boundaries of metamorphic facies do not coincide with stratigraphic contacts (Zhangurov, 1984).

In the neighboring Finnish territory, the metavolcanics of the greenstone belt are intruded with granitic plutons accompanied with pegmatites. The isotope age of the granites is around 1.9 Ga (Lehtonen *et al.*, 1985). The granitic intrusions correspond to the period of the folding and faulting. Various dikes (subalkaline granites, granodiorites, and later gabbrodiabases) intruded along steeply dipping faults.

Muscovite-rare metal and ceramic pegmatites are common in the Svecofennian tectonomagmatic cycle both in Karelia and in eastern Finland. They occur partly in the Lapland–Karelian greenstone belt as well. However, the most important for the regional metallogeny of this cycle are massive sulfide deposits, for example, Outokumpu, which has a high gold content (Gaall and Sundblad, 1990).

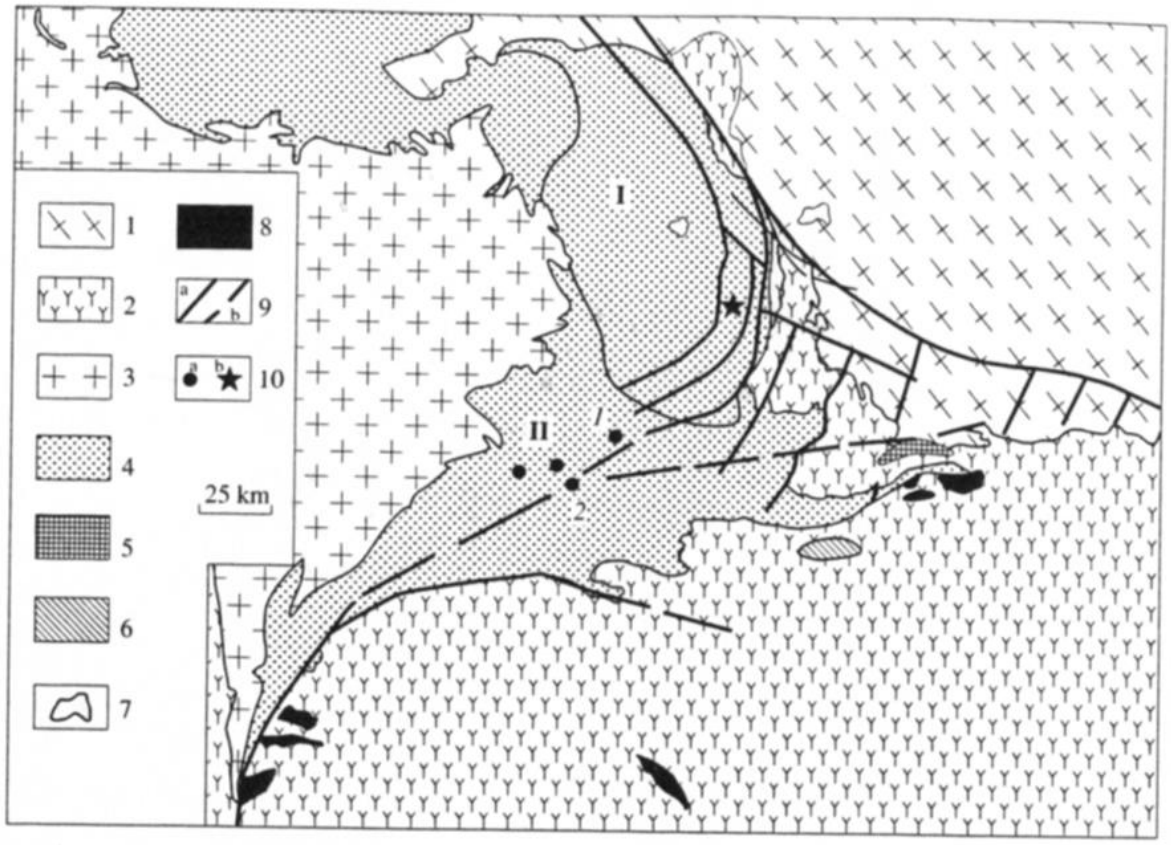

Fig. 2. Tectonic sketch of the Salla–Pana–Kuolajarvi part of the Lapland–Karelian belt (data of Ward *et al.* (1989) are used): (1) Granulites and gneisses of the Belomorsk megablock; (2) late Archean granitoids of the Karelian megablock (2725–2695 Ma); (3) Svecokarelian Early Proterozoic granites (1880–1770 Ma); (4) greenstones; (5) charnockites; (6) potassic granites Nuorunen (2450 Ma); (7) Paleozoic alkaline granite small intrusives Sallantva and Vuorijarvi (380 Ma); (8) differentiated initially layered peridotite–gabbro-norite intrusives (2340–2400 Ma); (9) deep-rooted faults: (a) observed, (b) inferred according to geophysical data; (10) gold deposits: (a) gold–sulfide (disseminated): (*1*) Juomasuo, (*2*) Konttiaho; (b) quartz gold vein Maisk deposit; (I) Salla–Kuolajarvi structure; (II) Kuusamo–Paanajarvi structure.

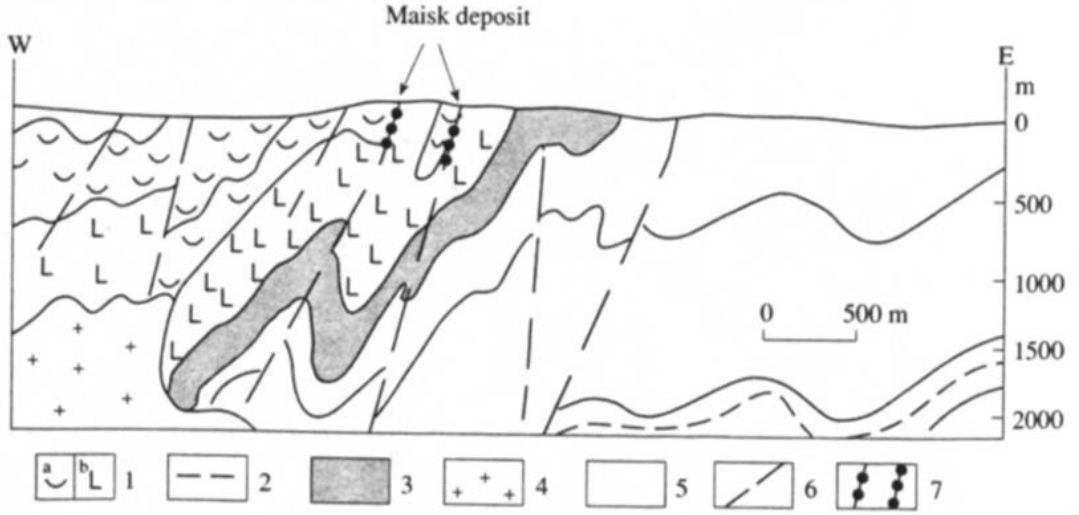

Fig. 3. Schematic geological cross section of the eastern part of the Kuolajarvi structure. (1–3) Early Proterozoic rocks of the Kuolajarvi structure: (1) upper tuffogenous (a) and middle effusive (b) sequences; (2) carbonaceous tuffoschists; (3) ultrabasic; (4) unexposed granites; (5) Early Proterozoic volcanic and metasedimentary rocks; (6) regional faults; (7) ore-bearing faults.

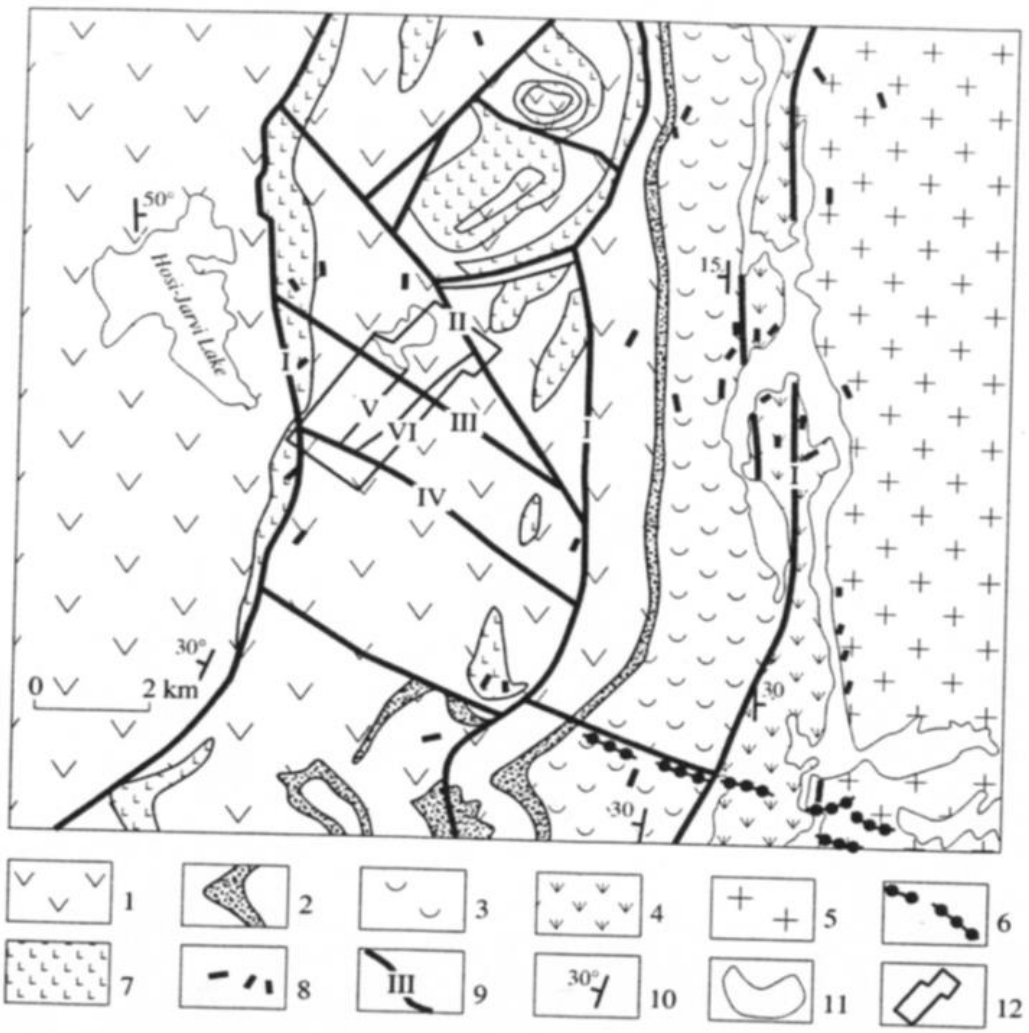

Geologic scheme of the Maisk deposit district (data of the Central Kola Prospecting Enterprise are used, with additions). Early Proterozoic: (1) metabasalts of the Aapajarvi suite, (2) conglomerates and sandstones of the Noukajarvi suite, phibole schists, graphite-bearing fillitic schists, metasandstones, and dolomites of the Sovajarvi series, (4) amphibole pla- sts, mica–quartz schists, and quartzites; (5) Late Archean granodiorites, plagiogranites, diorites, and plagiomicroclinic gran- vajarvi association); (6, 7) intrusive rocks of the Kalevian age: (6) olivine gabbro–diabase dikes (Jatulian–Ludikovian), agabbro–diabases, metagabbros, and metagabbro–pyroxenites; (8) quartz veins; (9) faults: (I) main faults bounding the gra- ncline, (II) the northern interblock fault, (III) the central interblock fault, (IV) the southern interblock fault, (V) the western ring fault (vein zone no. 1), (VI) the eastern ore-bearing fault (vein zone no. 40); (10) strike and dip of host rocks; (11) lakes; undaries of the Maisk ore field.

relia, massive sulfide bodies are common, but no deposits of economic interest. However, occurrences of antimony and arsenic miner- are known there (Rybakov *et al.*, 1993). Gold ation occurs in the Kuolajarvi region and in ern end of the greenstone belt together with nineralization.

gold and sulfide–gold dissemination is com- he Salla–Kuolajarvi structure, but economic occur only at the Maisk deposit. The –Paanajarvi structure contains the small lfide gold deposits Juomasuo and Konttiaho. ologists relate the genesis of these deposits to an tectogenesis, as in the case of the most rep- resentative deposits in the Nordkalott region of the Lapland belt. The Suurikuusikko deposit was found there recently. Its reserves exceed 50 t of gold with an average content of 6 g/t (Fig. 1). The deposit consists of a large vertical mineralized zone within the regional fault. The length of the zone exceeds 5 km, and its width varies from 1 to 60 m. The zone is localized along the contact between magnesian and ferrous toleitic metavolcanics containing graphitic tuffites, siliceous schists, and apokomatiite schists. Graphite veinlets and products of carbonatization and asbestosization are common in the mineralized zone. Numerous lenslike or veinlike orebodies are situated at intervals rich with veinlet–disseminated sulfides (pyrite, arsenopyrite, and gersdorffite). The ores contain hard-to-extract "invisi-

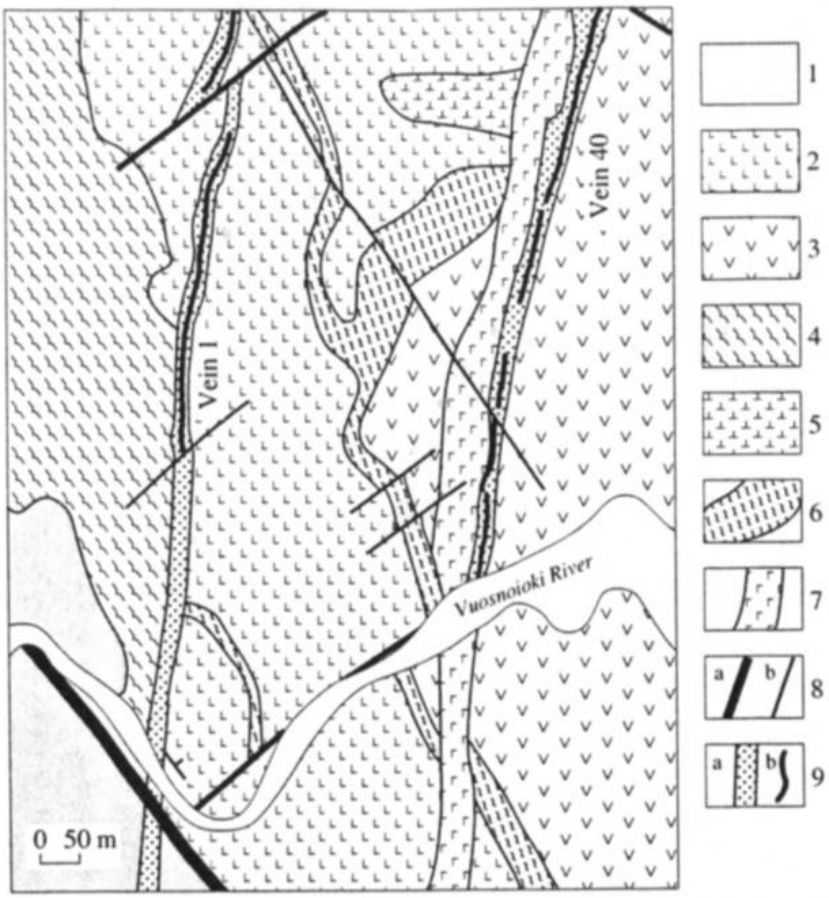

Fig. 5. Simplified geological map of the Maisk deposit (based on data of the Central Kola Prospecting Enterprise and the authors). (1–4) Aapajarvi suite: (1) carbonate–chlorite–tremolite schists, (2) metabasalts, (3) tuffoschists and tuffolavas, (4) the first layer of metabasalts; (5) metadiabase sills; (6) the second layer of tuffoschists; (7) serpentinites and metagabbro–pyroxenites; (8) faults: (a) large and (b) small; (9) (a) ore zone and (b) quartz veins.

ble" gold, only 5–7 wt % of which is free. The rest is enclosed in arsenopyrite (around 70 wt %) and in pyrite (around 20 wt %). The gold content in arsenopyrite reaches 2800–2900 g/t and in pyrite, tens of grams per ton. The age of the deposit is 1850–1890 Ma.

Some small gold deposits occur in this region as well. Among them, the Pahtavaara deposit contains visible gold with high fineness (990‰) enclosed in biotite–amphibole–barite–quartz–carbonate veinlike bodies (Fig. 1).

The komatiitic metavolcanics and ultrabasic (?) host rocks of the deposit underwent listvenitization (formation of the metasomatic quartz + carbonate + pyrite + fuxite assemblage), which was followed by the quartz–amphibole mineralization with pyrite, magnetite, and gold. The isotopic Pb–Pb age of pyrite and magnetite is 1810 Ma.

GEOLOGICAL DESCRIPTION OF THE MAISK DEPOSIT

The Maisk deposit consists of gold-bearing quartz veinlike bodies. They correspond to the splitting–shear structural type of ore zones. The two vein zones are mapped and prospected there. They occur within intrablock faults striking NE (Fig. 4). These faults are limited from the N and S by latitudinal interblock faults, which, in turn, conjugate at the W and E with the main arclike faults bounding the Kuolajarvi graben–syncline. Two closely spaced intrablock ore-localizing faults strike NE, having a length of more than 2.5 km and a width of up to 100–150 m. The distance between faults is 300–400 m (Fig. 5). The faults steeply dip to the NW at an angle of 60°–80°. They divide the deposit area into three parts: eastern, middle, and western. The middle part is descended and shifted to the SW relative to the other parts. The amplitude of the shift is around 250–300 m.

The ore-bearing faults are crossed and shifted by latitudinal and NW faults. Strongly destroyed is the western ore-controlling fault, whose fragments are shifted to the E or W for a distance of 40–50 m.

The host rocks of the deposit relate to two age groups: pre-Svecofennian (riftogenic) and Svecofennian (orogenic). The rocks of the first group consist of metabasalts (Aapajarvi suite) and tuffogenic-sedimen-

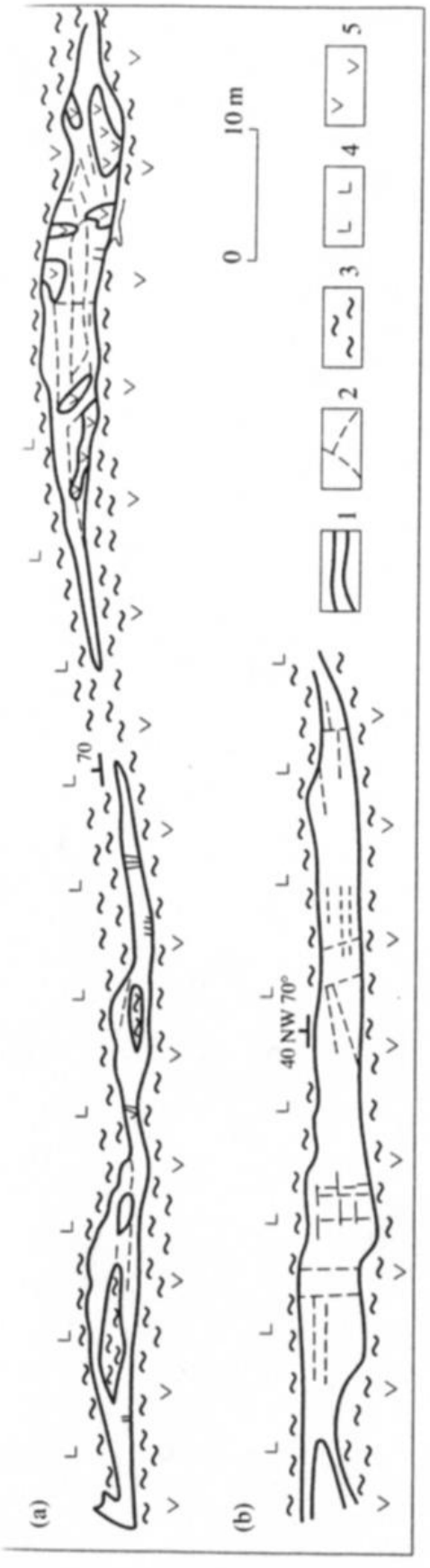

lorphology of (a) vein 1 and (b) vein 40. (1) Quartz; ring; (3) amphibole and talc schists; (4) metapyrox- 5) metabasalts.

tary rocks (Kailar suite). They are intruded by sills and dikes of gabbrodiabases and by gabbro–pyroxenite sills. The Svecofennian rocks are folded and metamorphosed under intermediate conditions between greenschist and epidote–amphibolite facies. The fold axes are oriented NNW. The Kalevian gabbrodiabase dikes localizing in the ore-bearing faults relate to this Svecofennian group.

The ore-bearing faults form narrow shear zones of rock milonitization and brecciation. Their width reaches 10 m, but is commonly 5–6 m. Faults of different orientation are barren. Gold is very irregularly distributed inside quartz bodies and forms ore shoots.

Two parallel NNE fault zones, containing quartz gold veins no. 1 and no. 40 (Fig. 5), are distinguished and explored along strike to 1.6 and 1.7 km, respectively. They are usually explored to the depth of 100 m, but by some boreholes, to 150 and 300 m. Vein zone no. 1 (the western one) contains vein nos. 1, 25, and 41. At the surface in vein 1, an ore shoot was found. It has a length of 110 m and an average gold content 13.1 g/t (the highest content is 266 g/t). The parameters of vein nos. 25 and 41 are not estimated. The ore shoot in the eastern vein zone, no. 40, has a length of 80 m at the surface and an average gold content of 10.5 g/t. Ore shoots have a bandlike shape (studied to a depth of 20–30 m) and gently plunge (15°–20°) to the NE.

Vein 1, exposed in the wall of the open pit, coincides with the orebody boundary and has sharp tectonic contacts. Pocketlike and veinlet sulfide mineralization occurs in the vein selvages and at the rock xenolith contacts with the vein quartz. The ore shoots in vein nos. 1 and 40, mined from the surface, occurred in NE faults, in places of their intersections with meridional tectonic zones (Fig. 5). The zones contain veins with complicated morphology, strongly fissured and rich with rock xenoliths (Fig. 6). The pyroxenite sills probably form structural barriers, under which the ore shoots were deposited.

The pyroxenites underwent the most intensive dynamometamorphism and are converted into finely schistose aggregates in the ore zones. The schistosity is directed along the zone strike or at a sharp angle to it, and pyroxene and amphibole crystals are elongated in the same direction. The host metabasalts are schistose only within the ore-bearing zones. The degree of their schistosity is strengthened in places to microfolding. The schistosity in metabasalts appears as a linearity in the orientation of metamorphic biotite, amphibole, and talc grains that coincides with the ore zone strike as a whole. The drag folds in the SW part of the footwall of ore zone 40 reach 10–20 cm. The folding was associated with shear deformation, while the footwall was shifted to NE, according to the fold joint morphology. The degree of rock deformation decreases with distance from the ore zones.

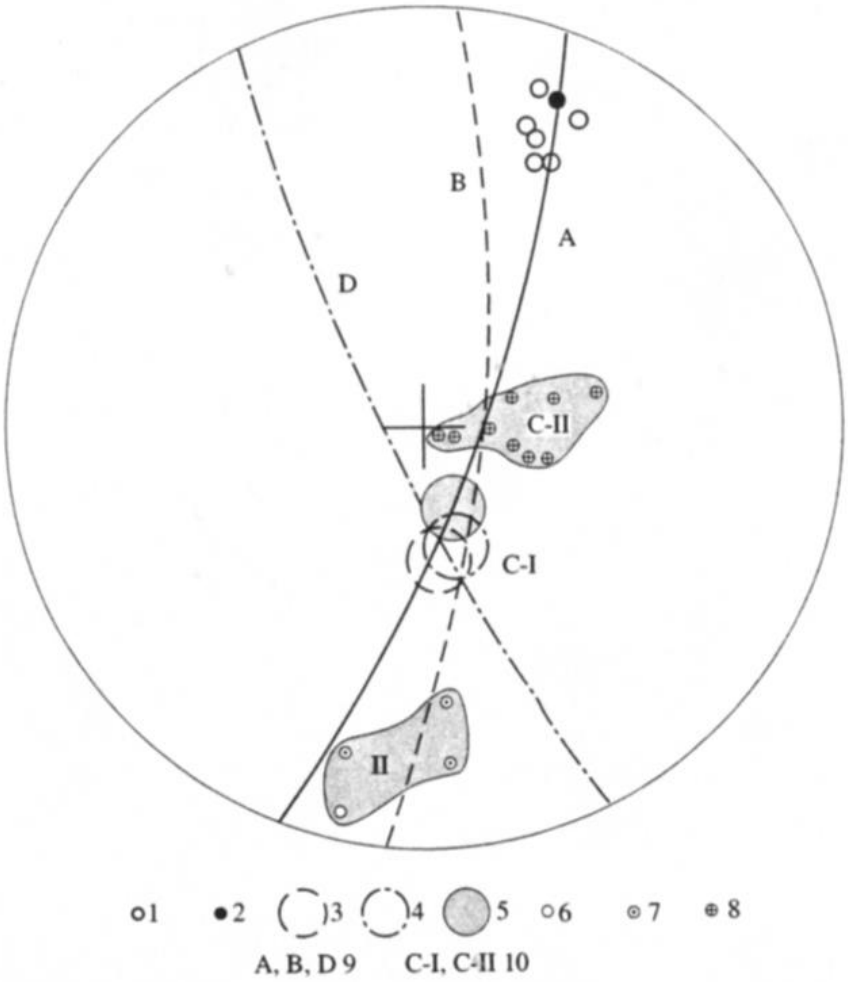

Fig. 7. Stereogram of the structural components. (1, 2) Slickenside grooves in quartzes 1 and 2, respectively; (3) axes of quartz veinlet intersections; (4) axes of fissure intersections in rock fragments enclosed in the quartz veins; (5) axes of fissure intersections in quartz; (6, 7) superposition of the slickenside grooves of the first (6) and second (7) generation in quartz; (8) bends of small folds; (9) average strike and dip parameters of (A) vein no. 40, (B) schistosity in the vein exocontact, and (D) host rocks; (10) deformation axes (C-I and C-II).

In addition to the described internal vein structure, the complicated tectonic evolution of the ore zones is evidenced by the occurrence of deformed host rock xenoliths (Fig. 6). Two xenolith types are distinguished: with massive texture and with complicate texture including fragments of fine structural forms. Some relics of small folds, inherited fissures, and quartz veinlets occur in metabasalts of the ore zone nos. 40 and 1. The fold axes are horizontal and coincide with the vein strike. Small folds have dimensions of some tens of centimeters. In addition, sheared metapyroxenites are observed in zone no. 1. The study of these relic forms suggests that the main compressive stress was oriented subhorizontally and that shear deformations in ore veins were simultaneous with the formation of quartz bodies in the ore-controlling faults.

The tectonic movements along vein zone nos. 1 and 40 continued after quartz deposition according to studies of ore shoots of these zones. The orientation of slickenside grooves in quartz (vein no. 40) corresponds to two stages of oblique-slip deformations (Fig. 7). This stereogram shows the orientation of the early slickenside grooves in quartz (1) and of the axis of the wavelike bended chloritized slickenside surfaces (2) in the hanging vein wall (Fig. 7). The bends correspond to the reverse faulting with a minor slip component. In contrast, the slickenside grooves show mainly horizontal displacement with a minor vertical shift. Such slickenside grooves could be formed upon shear deformations with the axis localized in the hanging vein contact toward the vein dip with a slight inclination to the north. The B axis had the same position in the process of formation of the quartz bodies, according to measurements of the intersection of the quartz veinlet axes (3-B_1) and fissures in the rock xenoliths in quartz (4-B_1). Fissure intersections in quartz have the same orientation (5-B_1). The slickenside grooves of generation I are overlapped with the slickenside grooves of generation II, which

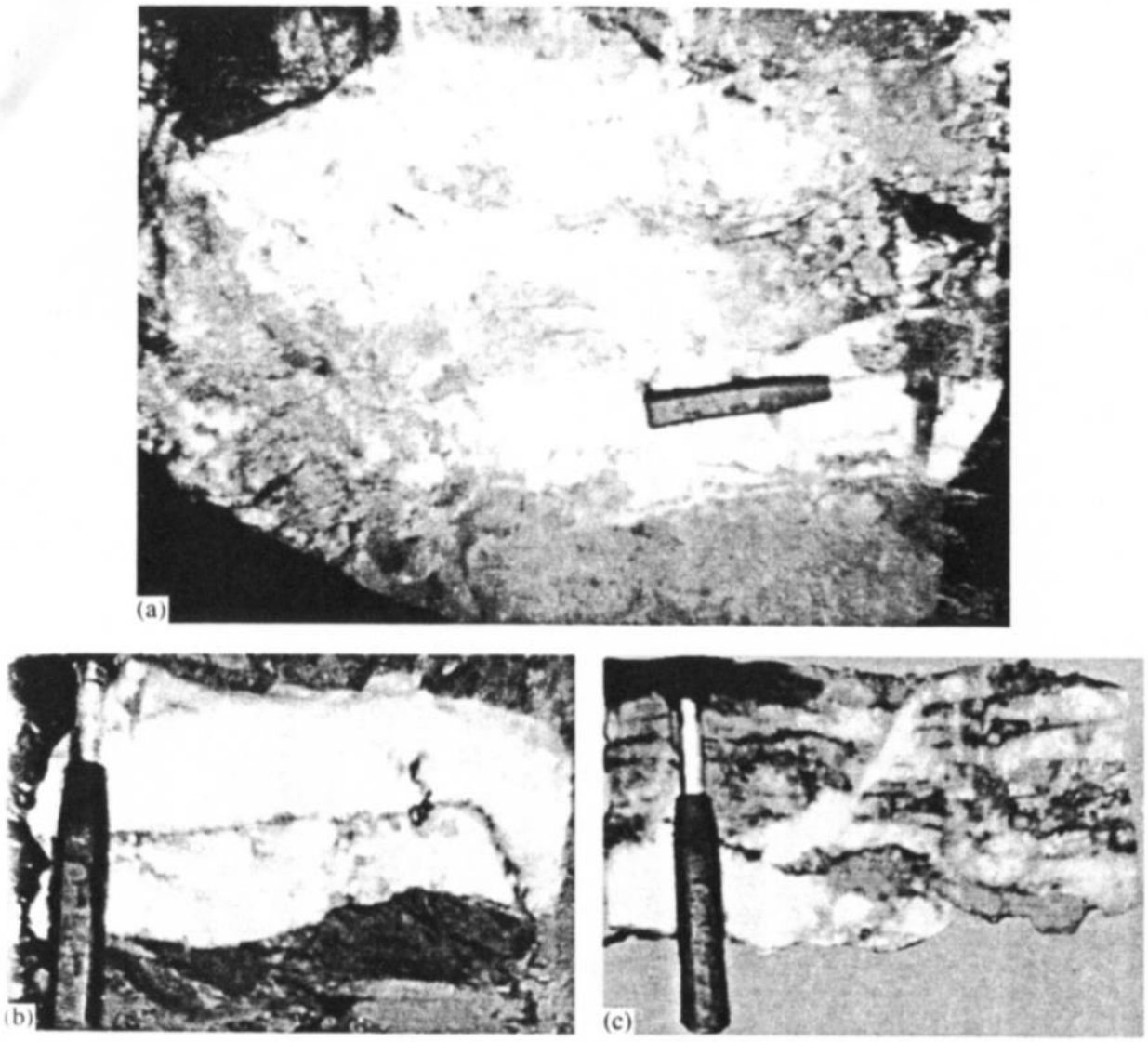

. 8. Textures of quartz veins at the Maisk deposit: (a) breccia texture, fragment of vein no. 1 from the open pit; (b) banded texture, ;ment of quartz vein no. 40 from the open pit; (c) banded texture, fragment of vein no. 40 from the open pit.

in quartz (6) and in the host schists (7). The defor- axis (B-II, 10) of the late stage is distinguished schistosity bending and in bends of some small like folds (8). Slip movements along the late nsides had an opposite direction relative to those first stage. These data explain the complicate dis- on of the ore shoots within ore zones. The gentle of ore shoots to the NE is possible in the case of overthrusting in the ore zones, which caused the ion of the wavelike surface bends in quartz.

ORE FABRICS

e orebodies of the Maisk deposit have a uniform sition. Biotite, calcite, amphibole, chlorite, oligoclase, and accessory apatite and sphene there in addition to quartz. The main ore minerals se less than 1% of the vein. They are (in order of sing abundance) chalcopyrite, pyrrhotite, sphalerite, galena, and native gold. The subordinate and rare minerals are mackinavite, pentlandite (Co variety), lead and bismuth tellurides (altaite and tsumoite), galenoclaustolite, costibite, magnetite, pyrite, and marcasite. Other authors noted cubanite, bornite, tellurobismuthite, and klockmanite (Gavrilenko *et al.*, 1999). Monomineral aggregates of chalcopyrite and its intergrowths with pyrrhotite, amphibole (grunerite), sphalerite, galena, and sometimes with gold are the most common in veins. The oxidation zone is poorly developed.

Massive quartz composes the groundmass of the ore, and the ore fabric depends mainly on relations between quartz and various altered rock xenoliths. Xenoliths occur mainly in the SW part of zone 1 (Figs. 6, 8a) and have an oval shape. The dimensions of xenoliths vary from some centimeters to some meters. Their occurrence is near to conformable with the vein strike or diagonal (Fig. 6). Metabasalts, containing

quartz veinlets, predominate in xenoliths. Such veinlets in pyroxenites are scarce.

A breccia fabric is typical for the vein selvages (Fig. 8a), where elongated plates of altered metabasalts occur. The latter are replaced with amphibole and biotite. These plates were separated from host rocks without any removement or rotation. The breccia texture of the vein varies along the strike and dip and depends on the degree of rock disintegration to blocks. Such a texture is commonly associated with the banded one (Fig. 8a) as a result of intensive rock disintegration in the quartz vein.

The banded fabric encloses relics of the schistose metabasalts and pyroxenites. The width of the rock plates varies from 0.1–1 to 5–10 mm (Figs. 8b, 8c). Quartz veinlets also vary in width. The appearance of the banded veins depends on the volume relations between quartz and inclusions. In places where the ratio exceeds 5, a massive central zone without banding and a banded zone near vein contacts occur (Fig. 5c). Such texture is common in widened intervals of the veins, where banding occurs throughout the vein. The metabasalt inclusions there commonly are replaced with thin-grained aggregates of albite, actinolite, grunerite, shamosite, and biotite with sulfide pockets and veinlets. Aggregates of amphibole and chlorite are the main constituents of the banded fabrics (Figs. 8b, 8c). The micrograined aggregates of other minerals are gradually change to vein quartz. The transitions of the banded veins to systems of thin veinlets and varieties of texture (number of bands, distance between them, and combinations with breccias) are a result of rock replacement and mineral deposition from solutions in parallel fissures. In some places in veins, nets of quartz veinlets occur. Veinlets in nets are oriented either along veins or perpendicularly to their contacts. The perpendicular veinlets cross the vein banding but do not cross vein contacts (Fig. 8c). Such veinlets at the Bendigo deposit are called "quartz teeth" (Sharpe and McGeehan, 1990). The quartz in the quartz teeth is similar to that of the vein.

Ore minerals form disseminated or veinlet–disseminated textures. The veinlet width is 1 cm or less, and the length is 10–20 cm. Sulfide pockets some centimeters in diameter occur in the vein endocontacts. Pocket–dissemination textures in some places are formed by the amphibole distribution (with or without albite).

MINERAL COMPOSITION OF ORES

Quartz is the main gangue mineral. It is milky white or gray and fine-grained, and its grains have complicate shape. Most of the vein quartz relates to the first (the early) generation. Calcite pockets some centimeters in diameter associate with this quartz. Calcite is twinned and intergrows with quartz.

Quartz II is a result of recrystallization of the early quartz. It is granulated, fine- to medium-grained, and has a gradual transition to the early quartz. The granulated quartz occurs only in ore shoots. It is grayish o brownish due to biotite, amphibole, and possibly k feldspar inclusions.

The X-ray–fluorescent analysis indicates som admixtures in the monomineral fraction of the gold bearing quartz from ore shoot 1: in wt %: Cr_2O_3 (0.001–0.002); MnO (0.005); TiO_2 (0.02); MgO (0.14); Al_2O (0.25); Na_2O (0.14); and K_2O (0.01); in g/t: Ba (3–4) Co (2–3); Ni (7–10); Cu (1–12); and Zn (2). These samples, with 96–99 wt % of SiO_2, strongly differ from those containing thin inclusions of other gangue minerals and a significantly lower amount of silica (63–76%). The latter samples are enriched by 1–2 orders in the components listed above. These components are established in barren quartz (0.005–0.086 g/t Au) as well, showing similar content. In samples enriched with K_2O (0.03–0.26%) but with less Na_2O (0.03–0.06%), the Co content decreases by an order and the Ba content increases to 16–37 g/t.

Fine- to medium-grained quartz I aggregates containing pockets of albite, amphibole, and biotite are common in banded veins together with some pegmatitic-like quartz–albite–amphibole aggregates. The latter occur in the SW end of vein no. 40 and consist of large, well-oriented quartz crystals up to several centimeters wide and forming nests 10 × 10 cm in size. Interstices between quartz crystals are filled with albite and small biotite flakes. Amphibole occurs at the base of the crystal druse hosted by granulated quartz of the ore root in vein no. 1. The biggest quartz crystal has a length of 10 cm and the cross section of 4 × 4 cm. Fine-grained amphibole (grunerite) partly covers quartz planes. It commonly associates with sulfides and rarely with gold, as does chlorite.

Ore minerals (pyrrhotite, chalcopyrite, sphalerite, and galena) occur together or separately in the same places of veins. The minerals either fill interstices between quartz grains or form thin discontinuous veinlets crossing quartz. Sphalerite (Table 1) is disseminated and forms pockets. It commonly contains emulsion of chalcopyrite and pyrrhotite. Pyrrhotite forms small crystals disseminated in quartz and replaced with pyrite and marcasite. In some pyrrhotite grains, as in chalcopyrite grains, cleavage is distinguished, indicating that these minerals have not undergone strong deformations. Magnetite occurs together with pyrrhotite and chalcopyrite as small grains. All these minerals associate with amphibole (grunerite); however, only chalcopyrite forms close intergrowths with it (Fig. 9). Chalcopyrite predominates over other ore minerals and forms pockets, veinlets (0.001–0.8 mm wide), and minor inclusions (0.002–12 mm) in vein quartz. It intergrows with galena, pyrrhotite, and rare gold. Mackinavite occurs in chalcopyrite grains as tiny braids. Pentlandite, containing 20–22% Ni, is rich with Co (~25 wt %). It occurs in some pyrrhotite grains as plates and flamelike inclusions. Hypergenic malachite

Table 1. Ore mineral compositions at the Maisk deposit

No.	Minerals	Cu	Fe	S	Pb	Zn	Se	Te	Sb	Co	Ni	Bi	As	Ag	Cd	Au	Σ
		wt %															
1	Costibite		0.14	14.59		0.28	0.24		57.37	24.82	2.19		0.12	0.00	0.00		99.75
2	"		0.13	14.64		0.00	0.18		57.55	24.31	2.87		0.10	0.00	0.00		99.58
3	Sphalerite		7.19	33.31		55.16	0.06		0.00	0.27	0.00		0.00	0.00	1.98		97.97
4	"		6.05	32.97		57.27	0.00		0.00	0.18	0.00		0.03	0.00	1.25		97.75
5	Altaite		0.03	0.00	61.02	0.00	0.78	37.64	0.34					0.10			99.91
6	"		0.00	0.00	60.95	0.00	0.72	37.16	0.26					0.07			99.16
7	Tsumoite		0.00	0.00	12.58		1.01	39.21					0.00	0.00			100.18
8	Galena-clausthalite		0.00	8.99	81.58		8.35	0.61					0.00	0.00			99.53
9	"		0.00	9.91	81.35		8.25	0.49				47.38	0.00	0.04			99.60
10	Gold	0.21						0.00	0.00			0.00	0.00	8.10		91.06	99.20
11	"	0.04						0.00	0.00			0.26	0.00	6.57		92.83	99.85

Note: Analyses were performed with a Cameca XS-50 microprobe analyzer at IGEM RAS (analyst: A.A. Tsepin). Voltage, 20 kV; current, 20 nA; exposition time at the point, 30 s for Se, As, and Ag and 10 s for other elements. The software program RAR was used for recalculation of the concentrations.

and covellite in some places replace chalcopyrite. Galena intergrows with chalcopyrite, sphalerite, pyrrhotite, and rare gold and occurs separately in vein quartz as tiny allotriomorphic inclusions or veinlets. The sizes of galena grains and its aggregates are 0.001–1 mm, and 0.02–1.5 mm, respectively. Galena grains are commonly covered with thin crusts of iron hydroxides and anglesite.

Tellurides (altaite and tsumoite) are typomorphic minerals at the deposit (Table 1). They relate to the sphalerite–galena–pyrrhotite–chalcopyrite aggregates and intergrow with each other. Their grain size is less than 100 μm. They are especially common in galena and along its contacts. The galena-like mineral intergrowing with tellurides is rich with Se and its composition corresponds to clausthalite (Table 1). Costibite, a very rare mineral, was observed in intergrowths with chalcopyrite, sphalerite, and gold.

Gold is distributed very irregularly in quartz veins of the Maisk deposit. The highest gold contents occur in

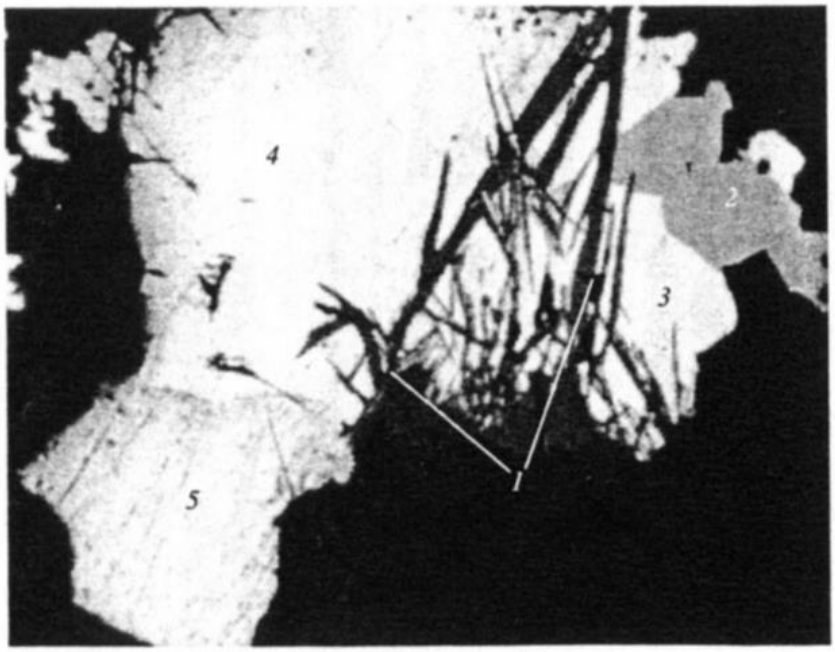

Fig. 9. Gold in the chalcopyrite–sphalerite–galena–grunerite assemblage (magnification 40). (*1*) Grunerite; (*2*) sphalerite; (*3*) chalcopyrite; (*4*) galena; (*5*) gold. The black background: quartz.

the ore shoot of vein no. 1, which was the starting point for prospecting of the deposit. The shoot contains some areas with heightened gold concentration. One of these is related to the xenolith of altered metabasalts 3 × 1.5 m in size. The other (1 × 1.5 m) is related to the footwall of the vein. Irregular, platy, rectangular, and rounded gold grains are 1–2 mm in diameter and sometimes form chains. They occur in fissures in quartz, in amphibolitized and chloritized relic rocks, and in places where sulfide dissemination and films are present. Visible disseminated gold occurs throughout the SW flank of vein no. 40. In this vein, near its contact, thin gold disseminations and films occur on the surface of quartz covered with spots of thin-grained chlorite. Three varieties of gold are distinguished there: (1) angular grains and crystals up to 1 mm in size intergrown with quartz; (2) small crystals and angular grains overgrowing quartz and hosted by amphibole; and (3) thin films covering slightly twisted fissure surfaces and slickensides. The movements that caused the slickenside formation were low-productive.

Commonly, gold forms irregular platy, rectangular, or rounded grains up to 1–2 mm in size and intergrowths with chalcopyrite and galena (Fig. 9). Dimensions of gold grains vary from 0.002 to 1 mm, but the most abundant is 0.02–0.1 mm. Gold inclusions in sulfides vary from 0.006 × 0.03 mm to 0.06 × 0.03 mm. The gold is of high fineness and has a constant copper admixture (0.02–0.21 wt %). Twenty-eight gold grains were studied with an electron microanalyzer, and in 27 of them the gold fineness was 900–930‰. One grain from the intergrowth with costibite showed a fineness of 575‰.

The deposition of gold and sulfides in the quartz veins relates to ore mineralization overlapping quartz I.

ALTERATION OF HOST ROCKS

The rock alteration is the most intensive in rock xenoliths enclosed in quartz veins and in rocks adjacent to vein contacts. The following types of altered rocks are distinguished: propylites overlapped on biotite–amphibole metamorphic rocks; early albitized rocks; magnesian metasomatites (Mg–Fe amphiboles, biotite, and chlorite); and alkaline metasomatic rocks (oligoclase, muscovite, and microcline).

Some authors relate amphibolization and biotitization exclusively to regional metamorphic events (Gavrilenko *et al.*, 1999) and biotite–oligoclase alteration, biotitization, and amphibolization—to the areal metasomatism. The following observations, however, allow these processes to be related to the ore deposition: (1) the postmetamorphic Kalevian dikes of gabbrodiabases underwent these processes and (2) metamorphic albite and hornblende were replaced by metasomatic minerals in amphibolites, pyroxenites, and early gabbrodiabases. Detailed petrological and geochemical study allows up to five or six of biotite, chlorite, and amphibole to be di

Amphibolites consist of albite and am 40%), chlorite (10–15%), and epidote (5 dote is irregularly distributed in slight metabasalts. Thus, it enriches the hanging tral part of vein no. 40. Epidote replace phenocrysts or more rare minerals in the and fills amygdules with quartz. As a resu matism, gabbrodiabase dikes consist of phenocrysts (from some tenths of a mill 1 mm), prismatic phenocrysts of diop 1.5 mm), and fine-grained groundmass (ep rite + albite).

The early albitization caused recrystall metamorphic tabular albite to aggregate grains with an "oak leaf" structure, which evident in the postmetamorphic gabbrodia

The biotite–amphibole metasomatite ore veins in amphibolites and dikes. Magn lite is the typical mineral of these rocks, by calcite and quartz as well. Amphibole compositional zonation. Their outer zon actinolite with 0.2–0.5 wt % Al_2O_3 and th MgO = 9 : 18, which can decrease to 7 : zone consists of hornblende with around and the ratio FeO : MgO = 18 : 10. This on the host rock composition and the int metasomatic processes; thus, some amphibole metacrysts are combinations mina hornblende with low-alumina actin

The biotite and amphibole metasom the deposit polymineral aggregates, zones veinlets of biotite and amphibole, which a the gabbrodiabase dikes.

Near ore veins, biotite–amphibole–oli lets with microcline, muscovite, calcit occur in dikes. Veinlets are 1–4 cm wi zonation: both amphibole and biotite vei goclase margins. They occur togethe biotite–actinolite veinlets. In polymineral sisting of microcline, muscovite, oligo calcite, and hyalophane, oligoclase is rep covite and microcline. Biotite of the biotit oligoclase veinlets has the ratio FeO : M which slightly but constantly differs from of the biotite–amphibole metasomatite 19 : 12).

Oligoclase veinlets 1.5–2.0 cm wide calcite–microcline selvages up to 5 mm the amphibole metasomatites. In the axial veinlets, sulfide veinletlike intergrowths rite with pyrrhotite (3–5 mm in size) occ forms there large (1.5–2.0 mm long an wide) tabular crystals with brownish cov the fissure plane. The selvages of vei white and consist of quartz calcite + mi growths hosted by oligoclase. Quartz f

Table 2. Gas chromatography data for fluid inclusions in quartz at the Maisk deposit

Sample no.	Components								
	μg/g			μmol/g			mol %		
	N_2	CH_4	CO_2	N_2	CH_4	CO_2	N_2	CH_4	CO_2
M-11	0.259	0.175	6.011	0.009	0.011	0.137	5.7	7.0	87.3
M-23	–	0.075	1.687	–	0.005	0.038	–	11.6	88.4
M-26	–	0.750	7.988	–	0.047	0.182	–	20.5	79.5
M-32	0.097	0.450	5.062	0.004	0.028	0.115	2.7	19.0	78.3

Note: Analyses were made at IGEM RAS (analyst: T.B. Zhukova).

grains in oligoclase 0.1 mm in size; microcline occurs as tabular isometric crystals 0.1–0.2 mm across; and calcite forms irregular grains 0.2–0.4 mm in size. A thin (0.1–0.3 mm) band of chlorite and quartz separates the feldspar veinlets from surrounding rocks. The rosy white fringes contain hyalophane (except of microcline), the BaO content of which is up to 12 wt %. Its crystals show oscillatory zonation due to alternating zones with BaO content varying from 5 to 11 wt %. The hyalophane together with muscovite, biotite and K feldspar (up to 1.7 wt % BaO) composes the abovementioned brownish cover on the oligoclase crystals. In this assemblage, two parageneses are distinguished: muscovite + K feldspar and hyalophane. Biotite in these veinlets is present in two varieties. The first one (grains 300 × 300 μm) corresponds in composition to biotite of the magnesian metasomatites and is relic. The second forms intergrowths with K feldspar, muscovite, and hyalophane. Along boundaries of the first variety, thin fringes of hyalophane (20–30 μm) occur. The second variety differs in chemical composition (0.5 wt % TiO_2 and FeO : MgO = 16 : 12) and small grain size (up to 30 μm).

A thin fringe of K feldspar with 7 wt % BaO was found at a contact between a sulfide veinlet and oligoclase. Probably, the sulfide veinlet was deposited before oligoclase replacement by hyalophane but after formation of the oligoclase veinlet with microcline fringe. The oligoclase veinlet contains rare small quartz and chalcopyrite grains and thin (0.1–0.5 mm wide) cross-cutting veinlets.

Two stages of the hydrothermal process at the deposit are distinguished as a result of mineralogical study of the quartz veins and altered host rocks.

The first stage corresponds to propylitization, quartz vein deposition, and magnesian metasomatism with extensive (near the veins—spotty but intensive) rock biotitization.

The second stage includes gold ore deposition. Ore minerals form two assemblages: early (pyrrhotite–chalcopyrite) and later (gold-bearing with sulfides and tellurides). The ore stage mineralization is accompanied with K feldspathic metasomatism, which corresponds to gumbeitization according to its mineral parageneses, which are similar to those described by D.S. Korzhinskii and then distinguished as gumbeite metasomatic association (Zharikov and Omel'yanenko, 1978). Gumbeites are common in rare metal and some gold deposits. At the Maisk deposit, gumbeites occur very locally but are quite distinguishable.

FLUID INCLUSION STUDY

Fluid inclusions (FI) were studied by microthermometric and gas chromatographic analyses in various quartz samples. The microthermometric measurements operated in the temperature interval from –196 to +600°C with a Linkam THMS 600 thermocryochamber connected with an MBI-15 microscope that was equipped with a long-focus objective (80×; Olympus) and a video camera. The measurement accuracy was ±0.2°C in the temperature interval from 0 to –196°C and ±1.5° C in the interval 0–600°C. The FI compositions and solution salinity were estimated with cryometry by fixation of the phase transition points in the process of FI heating after their freezing. The salt compositions were estimated by the eutectic melting temperature ($T_{m.e.}$), and the salt concentrations, by the ice melting temperature ($T_{m.i.}$). The results were interpreted according to Goldstein and Reynolds (1994). The homogenization temperature was given without pressure corrections and corresponds to the lowest possible temperature of mineral formation. The gas chromatography was performed with an LHM-8MD chromatograph; the carrier gas was helium, and the sorbent Polysorb. The pressure was calculated on the basis of microthermometric data for syngenetic inclusions of carbon dioxide–methane and water–salt compositions. The FLINCOR software (Brown, 1989) was used for calculations. The studied preparations were polished plates 0.2 mm thick prepared from 20 samples. More than 120 FI were studied from samples consisting of coarse- or medium-grained quartz. In plates from the samples M-11 and M-23, only quartz occurs, but samples M-26 and M-32 contain disseminations of sulfides, and sample M-54 contains disseminated gold.

The FI in analyzed samples contain 80–90 mol % of CO_2 and CH_4 (Table 2). The nitrogen (5–7 mol %) was

determined in two samples (M-32 and M-11). The water content was not determined, and thus the molar concentrations were calculated without water and correspond only to relative concentration ratios.

As a result of measurements, the samples containing disseminated sulfides show heightened methane content (19–20 mol %). It must be noted that the method deals with the total mass of FI in a sample, both primary and secondary.

The following results were obtained with microthermometric measurements of quartz and oligoclase.

Quartz veinlets in metabasalts. Three-phase inclusions (gas + solution + isotropic cubic solid phase) occur in quartz of these veinlets. Primary FI (less than 10 μm), pseudosecondary FI (15–20 μm), and secondary FI (15–30 μm) are distinguished.

The primary inclusions are scarce. Their homogenization temperature is T_{hom} = 470–436°C. They contain Na chloride solution with $T_{m.e.}$ = –27.9 to –21.6°C, which corresponds to a concentration of 29–28 wt % (Table 3).

Pseudosecondary FI are divided into three groups:

(1) FI with T_{hom} = 259–244°C, of Na chloride composition with concentration 30.7–29.3 wt %. The homogenization begins with halite dissolution and is completed with dissolution of gas.

(2) FI with T_{hom} = 260–248°C, of Na chloride composition with some higher concentration (35.3–34.5 wt %). The halite dissolution completes the FI homogenization.

(3) FI with lower homogenization temperature T_{hom} = 225–198°C. They contain $MgCl_2$ solution ($T_{m.e.}$ = –38.9 to –36.6°C) with concentration 33.2–31.7 wt % of NaCl equiv.

Secondary FI show varying quantitative relations between solution, gas, and solids. Thus, their T_{hom} and concentration cannot be determined. However, on the basis of some intermediate values, it can be suggested that T_{hom} was not higher than 150°C. The solution has Ca chloride composition ($T_{m.e.}$ = –56.9 to –55.6°C) and a concentration near to brine.

Quartz from the veinlet with actinolite. FI were studied in quartz near its contact with needlelike actinolite crystals. The most common are three-phase inclusions (solution + gas + isotropic solid phase) with varying quantitative relations between phases and monophase gas inclusions. Two-phase inclusions (gas + fluid) rarely occur. All of these FI have similar $T_{m.e.}$, varying from –43.9 to –35.8°C (Table 3), which corresponds to a Mg chloride solution with an admixture of some other cations. The melting in the two-phase FI is completed with dissolution of salt crystal hydrates. Thus, the concentration was lower than saturation, but higher than the eutectic one. This means the concentration was located in the interval of 35.3–21 wt % $MgCl_2$ equiv. The point of solid dissolution in three-phase FI was not estimated quantitatively, but is higher than that noted above. The homogenization of two-phase FI and pearance of the gas in three-phase inclusions spond to the interval 21–172°C. The gas inclusio tain low-density gas, and so they do not show an transitions.

The needlelike actinolite crystallized from high centrated chloride solutions with Mg^{2+} as the predo cation under a temperature of 220–170°C and rat pressure. The temperature at the beginning of ac crystallization could be higher, because the studied respond to the late stage of its crystallization.

Feldspathic veinlets. Two-phase primary F 10 μm in diameter were found in rounded qu grains and in oligoclase crystal heads from quar cite–microcline selvages and in late quartz 2 v with sulfides. In quartz 1, FI have T_{hom} = 352- (Table 3) and chloride composition, probabl Mg^{2+} as the predominant cation. The FI in plag have T_{hom} = 330–315°C and predominantly Ca c composition. The $T_{m.e.}$ in both cases is lower t temperature of the two-component system, so it i able that Na^+ and (according to the mineral co tion) K^+ and Ba^{2+} occur in the solution. The con tion of the solutions (22–21 wt %) is near to bri ferent FI with higher temperature, 370–346°C found in quartz 2. The solution of these FI has N ride composition and a lower concentration, 11– (Table 3). The syngenetic two-phase gas FI low-density CO_2 (T_m = –58.8 to –58.1°C; homo tion was not observable), which indicates that t eral was deposited in an open system. These dat that the quartz–calcite–microcline selvage a quartz–sulfide veinlet were formed from vario systems. Therefore, two assemblages with qua be distinguished in feldspar veinlets. The first corresponds to gumbeites, and the other to the e quartz–chalcopyrite—pyrrhotite stage.

Quartz without gold and sulfides from vei and 40. (Samples M-11 and M-23; nos. 11, 12. in Table 3.) The following types of fluid inclusio found in quartz: (1) two-phase gas (40–50 v solution with T_{hom} = 355–301°C; (2) monoph syngenetic with FI of the first type; (3) three-ph (less than 10 vol %) + solution + cubic solid pha T_{hom} = 178–151°C; and (4) two-phase gas (le 10 vol %) + solution with T_{hom} = 143–116°C these FI types are found in the form of both prim secondary FI. The $T_{m.e.}$ for all of the studied F within the interval from –20.6 to –32.3°C, whic sponds to the system NaCl–H_2O. The solution tration strongly varies. The FI of type 1 with 350–300°C (nos. 11 and 12 in Table 3) have a tration of 7–3 wt %. The phase transitions und ing to –196°C were not observed in such F monophase FI syngenetic to them (type 2). This FI contains gaseous low-density H_2O–CO_2 flu an admixture of methane and nitrogen accordin data of chromatographic analysis (Table 2). Th

Table 3. Microthermometric data for fluid inclusions in minerals at the Maisk deposit

No.	*n*	T_{homCH_4}, °C	T_{mCO_2}, °C	T_{homCO_2}, °C	CH_4, mol %	$T_{m.e.}$, °C	$T_{m.i.}$, °C	T_m of the last crystal, °C	The main salt	*C*, wt % equiv NaCl	T_{hom}, °C	*P*, bar
The quartz vein in metabasalt												
1	5					–27.9…–21.6		135–114	NaCl	29.1–28.5	473–436	
2	7					–29.5…–22.1		175–140	NaCl	30.7–29.3	259–244	
3	5					–28.4…–23.8		269–248	NaCl	35.3–34.5	260–248	
4	7					–38.9…–36.6		225–198	$Mg(Na,K,Ca)Cl_2$	33.2–31.7	225–198	
5	6					–56.3…–53.4		–22.3…–21.8	$Ca(Na)Cl_2$	42.7–30.2*	<150	
Quartz from the veinlet with actinolite												
6	8					–43.9…–35.8		–25.8…+26.7		>35.3–21.0**	221–172	
Feldspathic veinlet												
7	3					–37.4…–36.7	–19.0…–18.5		$Mg(Na,K,Ca)Cl_2$	21.7–21.3	352–349	
8	6					–56.9…–55.6	–23.8…–22.6		Ca(Na,K,Mg,Ba) Cl_2	22.3–21.7*	330–315	
9	5					–25.2…–23.5	–7.5…–5.2		NaCl	11.1–8.1	370–346	
10	4		–58.8…–58.1	Not observable								
Quartz without gold and sulfides (samples M-11, M-23, and M-54)												
11	10					–25.1…–21.8	–4.9…–0.8		NaCl	7.7–1.4	>350–321	
12	7					–24.9…–20.6	–4.1…–1.4		NaCl	6.6–2.4	355–301	
13	11					–30.5…–26.0		178–151	NaCl	35–30	178–151	
14	18					–32.3…–23.8	–19.0…–6.1		NaCl	21.7–9.3	143–116	
Quartz syngenetic with disseminated sulfides (samples M-26 and M-32)												
15	4		–67.0…–65.7	–46.7…–35.2	70–62							520–500
16	2					–65.8…–64.7	–28.8…–26.3		$CaCl_2$ (+NaCl?)	24.5–23.4*	194–201	
17	1	–103.9			100(+N_2 ?)							
18	3		–66.2…–66.0	–40.7…–39.9	59–58							680–660
19	5					–66.9…–66.6	–24.7…–23.5		$CaCl_2$ (+NaCl?)	23.0–22.5*	208–191	
20	8					–66.2…–56.6	–31.3…–24.7		$CaCl_2$ (+NaCl?)	25.5–23.0*	176–163	
21	6		–62.7…–60.8	–14.7…+0.6	25–16							940–830
22	3						–3.4…–2.9		?	4.8–5.6	272–259	
Quartz with gold (sample M-54)												
23	13					–66.5…–50.7	–38.8…–22.3		$CaCl_2$ (+?)	28–22*	198–140	

Note: No., number of the FI group; *n*, number of studied FI; CH_4, mol %: methane concentration in the CO_2–CH_4 fluid; T_m, melting temperature (m.e., melting of the eutectic (appearance of the first liquid); m.i., melting of ice; * wt % equiv $CaCl_2$; ** wt % equiv $MgCl_2$.

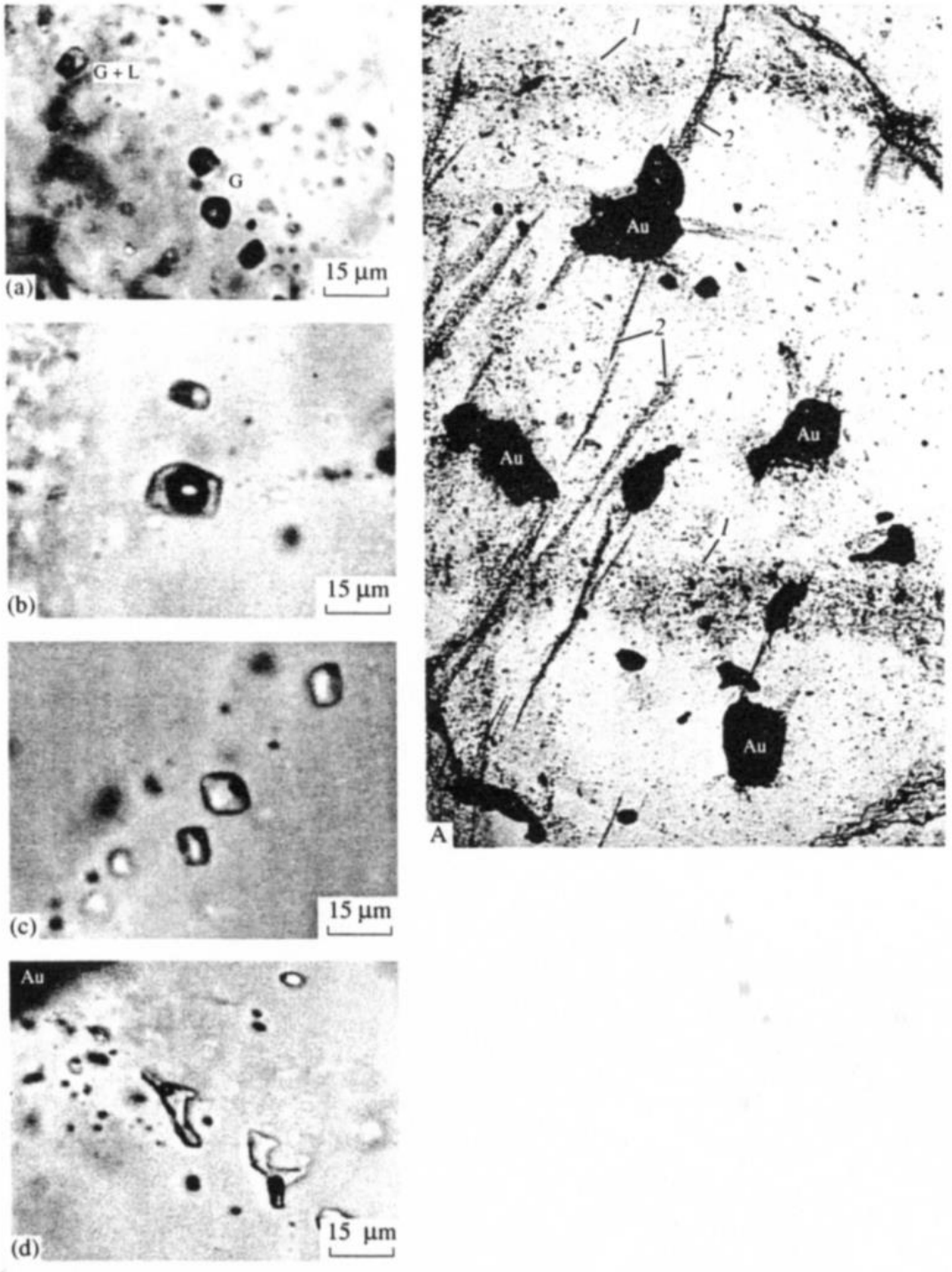

Fig. 10. Fluid inclusions in a quartz sample from vein no. 40 at the Maisk deposit. (A) Fissure systems in quartz (60×). oreless fissures; (2) later fissures, with gold (black), sample M-54. (a, b) Fissure system 1: (a) inclusion of NaCl solution and syngenetic inclusions with low-density fluids (G), (b) inclusion of NaCl solution (T_{hom} = 351°C; salinity, 4.6 wt %) L—solution); (c, d) fissure system 2 with inclusions of $CaCl_2$ solutions: (c) inclusions have T_{hom} = 192°C and a salinity of 2

rence of syngenetic FI composed of either solution or low-density gas is an evidence of fluid heterogeneity and proves that the pressure was not high in the process of mineral deposition. The FI of both types 3 and 4 have low gas content (less than 10 vol %). The concentration of FI of type 3 (three-phase, with solid phase, T_{hom} = 180–150°C) is 35–30 wt % and corresponds to brines (no. 13 in Table 3). FI of type 4 have T_{hom} = 1 and a concentration of 21–9 wt % (no. 14 in These FI types are divided by a temperature g not show transitional temperatures.

Thus, the quartz veins were formed from tw solution: high-temperature (350–300°C) highl

rated, with a low solution concentration (3–7 wt %), and low-temperature (180–116°C) water–salt solution with a concentration of 35–9 wt % and a low gas content. The description of the FI of various quartz generations follows.

Quartz syngenetic to sulfide dissemination. (Samples M-26 and M-32; nos. 15–22 in Table 3.) Some groups of primary FI with varying fillings were observed in the quartz crystals surrounding the sulfide grains: monophase vacuole and syngenetic to them two-phase gas (less than 20 vol %) + solution FI. Rare FI have mixed composition. The monophase FI turned to ice, and they began to melt at –67.0 to –60.8°C, which is significantly lower than the triple point of CO_2. The homogenization occurs in the interval from –46.7 to +0.6°C into liquid phase. Thus, the FI studied contain liquid CO_2 and some methane according to the above data. The FI group nos. 15, 16, and 20 (Table 3) are listed in order of increasing distance from a chalcopyrite grain. Calculations show that, in this direction, the methane content in FI decreases from 70–62 to 25–16 mol %. The highest methane content was estimated in quartz adjacent to the chalcopyrite crystal. In this quartz grain, one inclusion (no. 17 in Table 3) was observed that homogenizes into liquid at T_{hom} = –103.9°C, which is somewhat lower than the triple point of pure methane. Thus, the inclusion contains methane with an admixture of other components. The two-phase aqueous FI (nos. 16 and 18 in Table 3) syngenetic to the CO_2–CH_4 FI with T_{hom} = 194–201°C have $T_{m.e.}$ = –66.9 to –56.6°C, which is lower than the eutectic of the $CaCl_2$–H_2O and $CaCl_2$–NaCl–H_2O systems. Probably, the solutions have more complicate composition, but the main constituent is $CaCl_2$. These inclusions have a concentration of 22–26 wt % CaCl equiv. The same composition was estimated in some secondary FI in small fissures around the chalcopyrite crystal. $T_{m.e.}$ was not estimated for FI group no. 22 in Table 3, with T_{hom} = 272–259°C (the concentration is in wt % NaCl equiv). The pressure was calculated for the following FI groups: nos. 15 and 16, 18 and 20, and 21 and 22 (Table 3). The total interval of pressure values is from 500 to 940 bar. There is a trend of decreasing pressure toward the chalcopyrite crystal from 940–830 bar to 500–550 bar, which corresponds to the lowering of the homogenization temperature from 272–259°C to 194°C. Therefore, sulfides were deposited at increasing methane concentration and decreasing pressure and temperature. The main solution constituent was $CaCl_2$, with a concentration of 22–26 wt %.

Quartz containing disseminated gold. (Sample M-54.) One quartz crystal 2.5 mm in diameter, containing disseminated gold, was chosen for study (Fig. 10a). The quartz grain is broken by two fissure systems, which extend into neighboring grains: fissures of system 1 (Fig. 10a), without sharp boundaries, are perfectly sealed, rather long, and orefree; fissures of system 2 are numerous, short, distinctly late, and contain gold grains. Fissures of both systems are marked with secondary FI. System 1 contains two-phase gas (around 50 vol %) + solution FI (Figs. 10a, 10b). These inclusions have T_{hom} from 321 to >350°C, $T_{m.e.}$ from –25.1 to –21.8°C, and $T_{m.i.}$ from –4.9 to –0.8°C, which corresponds to the NaCl solutions with concentration 7.7–1.4 wt %. No phase transitions were observed in the monophase FI syngenetic with them during the cryometric procedures. Parameters of these FI are basically identical to those of the high-temperature FI in barren quartz. Fissures of system 2 contain two-phase FI as well, but with gas occupying less than 10 vol % (T_{hom} = 198–140°C) (Figs. 10b, 10c). They have $T_{m.e.}$ = –66.5 to –51.2°C and $T_{m.i.}$ = –38.8 to –30.2°C. Thus, this was a $CaCl_2$ solution with a concentration of 22–28 wt % $CaCl_2$ equiv.

OXYGEN, CARBON, AND SULFUR ISOTOPES

The oxygen and carbon isotope composition was studied in samples of quartz and calcite from the ore shoots. The value of $\delta^{18}O$ for the vein quartz varies from +1.23‰ to 12.1‰, with the mean value from 10 analyses being +8.62‰. The value is similar to that in Finnish deposits (Nurmi *et al.*, 1991) and corresponds to the magmatic source of water in the hydrothermal fluid. The $\delta^{18}O$ of calcite from vein no. 40 is +24.40‰, which confirms its deposition from magmatic fluid at low temperature. The $\delta^{13}C$ in calcite from the same vein is +9.89‰, which also corresponds to the magmatic source of the fluid (For, 1989).

The isotopic composition of sulfur was studied in the main sulfides from quartz veins at the Maisk deposit: pyrrhotite, chalcopyrite, and galena. The $\delta^{34}S$ values for the early deposited pyrrhotite (+7.03 and +7.12‰) significantly differ from that for later sulfides. The $\delta^{34}S$ values in galenas and chalcopyrite vary in narrow limits from –1.93‰ to –2.96‰ inside the interval from –4‰ to +4‰, related to magmatic sulfur. It must be noted, however, that magmatic sulfur and sulfur extracted from magmatic minerals have the same isotopic composition (Ohmoto and Rye, 1979). The mean $\delta^{34}S$ value for gold deposits in the Finnish part of the Lapland belt is +3.79‰ (Manttari, 1995). The $\delta^{34}S$ in sulfides of the magmatic Cu–Ni deposits of the Baltic Shield varies from +2.4‰ to +3.4‰ (*Nickel–Copper...*, 1985). This suggests a general source area for the whole region and possible migration paths. As a whole, the sulfur isotope composition in sulfides of the Lapland belt is similar to that in the Archean Barberton greenstone belt (South Africa) (from +1‰ to +4‰), in the Flin Flon Proterozoic greenstone belt (Saskatchewan, Canada) (from +2.8‰ to +5.5‰), and in Archean gold deposits in Australia (from +1‰ to +4‰) (Manttari, 1995).

Table 4. Lead isotope composition in galenas

Sample no.	Isotopic ratios					Model age, Ma	
	$\frac{^{206}Pb}{^{204}Pb}$	$\frac{^{207}Pb}{^{204}Pb}$	$\frac{^{208}Pb}{^{204}Pb}$	$\frac{^{208}Pb}{^{206}Pb}$	$\frac{^{207}Pb}{^{208}Pb}$		
M-XI	14.0414 ± 6	14.8633 ± 7	33.8858 ± 16	2.41323 ± 4	1.05852 ± 2	2538	
M-54	14.0461 ± 8	14.9140 ± 10	34.0511 ± 31	2.42421 ± 11	1.06179 ± 2	2615	1
M-36	14.0327 ± 9	14.8705 ± 10	33.9083 ± 25	2.41640 ± 6	1.05971 ± 2	2559	1
M-X	14.0318 ± 6	14.8884 ± 7	33.9695 ± 17	2.42087 ± 3	1.06105 ± 2	2589	1

THE AGE OF THE DEPOSIT AND SOURCES OF THE ORE SUBSTANCE

In this connection, the lead isotope composition in galena associated with native gold was studied. The galena shows small variations and primitive lead isotope composition (Table 4), with mean values (for four samples) $^{206}Pb/^{204}Pb = 14.0379 \pm 0.007$; $^{207}Pb/^{204}Pb = 14.88405 \pm 0.008$; $^{208}Pb/^{204}Pb = 33.9537 \pm 0.022$; $^{208}Pb/^{206}Pb = 2.41868 + 0.006$; and $^{207}Pb/^{206}Pb = 1.06027 \pm 0.002$. Thus, the modal age is 2575 Ma according to the Stacy–Kramer model. These data are in accordance with previous data (Turchenko *et al.*, 1991). The μ_2 value indicates the crustal lead source (Table 4).

The lead isotope composition at the Maisk deposit differs from those of other deposits in the Lapland Early Proterozoic greenstone belt according to comparison with the data of Finnish geologists (Fig. 11), but is similar to the isotope composition of the low-radiogenic Late Archean greenstone belts (Fig. 12).

The abundance of K-containing minerals in veins and ore-accompanying metasomatites, and their obvious relation to ore deposition allowed the fi isotope age data of the ore deposition at th deposit to be obtained (Table 5).

Two age groups of minerals are distinguishe ing to Table 5: around 1400 Ma and 1700–1900 degree of correspondence of these data to the is not clear. It is obvious that Ar loss took pla postore geological history of the region. Prob is the reason for the variations in isotopic data ples 7929 and 7930 (albite and biotite), collec the same metasomatic rocks. The post-albite biotite deposition of talc in the hanging wall o can be an additional reason for the variations i tope age data. However, a various time of a biotite deposition is possible in this part of th any case, the pre-Middle Proterozoic age of t thermal mineralization overlapping the quart confirmed.

The Rb–Sr isochrone age of the preore estimated for monofractions of the biotite (ples), amphibole (one sample), and albite (on The isochrone corresponds to 1610 ± 30 Ma

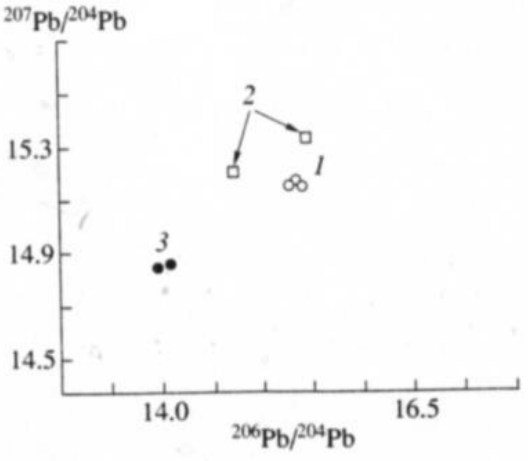

Fig. 11. Lead isotope compositions of galenas from the ore deposits of the Lapland Early Proterozoic greenstone belt (data for Finnish deposits are from Manttari (1995)). (*1*) The gold deposits Kuotko, Soretiavuoma, and Kiistala; (*2*) the Cu–Zn–Pb–Ni–Co stratabound deposits Riikonkoski and Pahtvuola; (*3*) the Maisk deposit.

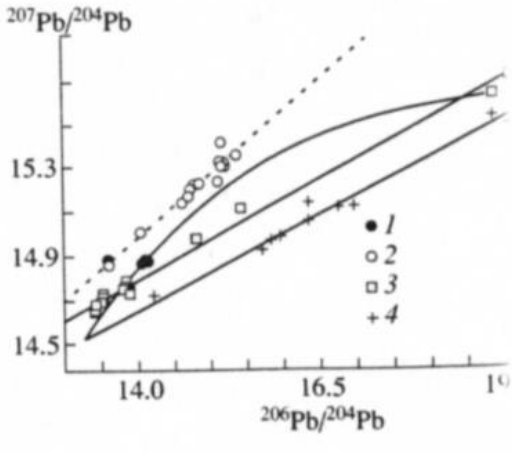

Fig. 12. Lead isotope compositions of the sulfide ization in the Late Archean to Early Proterozoic Finland (Vaasjoki, 1989). (*1*) The Maisk deposit deposits of the high-radiogenic group; (*3*) the de the low-radiogenic group; (*4*) the deposits of th greenstone belt (Canada).

Table 5. K-Ar age of metasomatic and vein minerals

No.	Mineral	M, % ±σ	$^{40}Ar_{rad.}$, ng/g±σ	$^{40}Ar_{rad.}$, % $^{40}Ar_{total.}$, %	Age, Ma ± σ
7329	Albite	0.83 ± 0.04	114.0 ± 2.0	51; 72	1380 ± 40
7930	Biotite	7.81 ± 0.06	1470 ± 20	90; 91	1710 ± 35
7968	Amphibole	0.042 ± 0.004	7.9 ± 0.6	36; 48	1700 ± 120
7932	Biotite	7.79 ± 0.06	1600 ± 40	86; 90	1810 ± 40
7931	Biotite	7.5 ± 0.06	1650 ± 25	67; 88	1880 ± 40
7928	K-feldspar	10.87 ± 0.1	1505 ± 20	91; 96	1380 ± 30

Note: Analyses were performed at IGEM RAS. Sample 7329, metasomatites near the vein; 7930, metasomatites after metabasalts in the hanging wall of vein no. 1; 7968, amphibole druse from vein no. 40; 7932, metasomatic zone near vein no. 39 in carbonate rocks (1 km SW of vein no. 1); 7931, metasomatites after carbonate rocks in the northwestern part of the ore district; 7928, microcline–quartz vein in Lower Proterozoic metavolcanic rocks in the eastern part of the district.
The content of radiogenic argon was estimated with an MI-1301 mass spectrometer by the method of isotopic dilution and with ^{38}Ar as the standard. The K content was estimated by flame spectroscopy (analyst: M.M. Arakelyants).

starting ratio $^{87}Sr/^{86}Sr = 0.7070 \pm 2$ (I_0). The Rb–Sr and K–Ar data are in good correspondence with each other and hence indicate the real age of the metasomatic process. Thus, the ore mineralization, which is younger than the wall rock alteration, cannot be older than 1610 ± 30 Ma. The I_0 is higher than the $^{87}Sr/^{86}Sr$ ratio typical for the mantle and is intermediate between mantle and upper crustal values. Therefore, in addition to Sr originating from the mantle, a significant fraction of Sr in the hydrothermal system came from an upper crustal source. The low-radiogenic Sr with mantle characteristics could be extracted from the ore-bearing basic rocks. The radiogenic Sr could be added from either the hypothetic crustal magmatic chamber or from Archean (2.5 Ga) metamorphosed volcano–sedimentary rocks, that occur in the Kuolajarvi trough. The latter is more probable, because no products of Late Proterozoic acid magmatism are known in the region.

The postore calcite shows some variations of the Sr isotope ratio (from 0.704 to 0.707). The reason for such variations is probably related to mixing of Sr inherited from host metasomatic rocks, with I_0 more than 0.707, and Sr introduced with the hydrothermal solution, with I_0 less than 0.704. The source area of the latter could be unaltered basic host rocks.

DISCUSSION

The Maisk deposit is one of the youngest hydrothermal gold deposits of the Baltic Shield according to results of this study and published data (Gaall and Sundblad, 1990; Sundblad, 1999). The formation of the deposit relates to the Late Svecofennian metallogenic epoch, which was widely developed in the Karelo–Finnish province (Rybakov *et al.*, 1993). However, the post-Svecofennian formation of the deposit is possible, as in the case of the Sohlstadt deposit in southeast Sweden (Sundblad, 1999). It must be noted that the boundaries of the Karelian (Svecokarelian) Early and Late Svecofennian epochs have various age limits within the interval 2.1–1.7 Ga. The Svecofennian epoch in the Karelo–Finnish region was rich with the formation of gold deposits and gold-bearing deposits of various metals: Cu + Zn, and partly Co + Pb + Te, Se; rarely + As (Boliden). The gold-bearing districts Nordkalott (in the northern part of Lapland) and Skelleftef (in northeast Sweden) have similar geochemical features. These deposits are related to the Svecokarelian metallogenic terrains, as is the Kuusamo region in the Salla–Kuolajarvi structure with small Au–Co–U deposits. The age of these deposits is 1.9–1.8 Ga, in contrast to that of Svecofennian deposits (1.8–1.7 Ga).

The Maisk deposit is the southernmost of the deposits with the Au–Cu–Pb–Te (Se) geochemical profile in the Lapland–Karelian greenstone belt. The Karelian branch of the belt is characterized by the Sb–As ore mineralization (Rybakov *et al.*, 1993).

Geochemical features of various ore districts in the Baltic Shield relate to various geodynamic regimes. The deposits in the Kuusamo region are synorogenic and paragenetic with granite magmatism (Pankka and Vanhanen, 1992). Deposits of the northern part of the Lapland belt also relate to synorogenic ones. They were formed by deep-seated magmatism and metamorphism. The difference in ore sources and formation conditions between them and the Maisk deposit corresponds to variations in the lead isotope composition. The similarity of galenas at the Maisk deposit to galenas at the deposits with low-radiogenic lead (Fig. 12) is probably caused by the relation of ore deposition in the eastern flank of the Kuolajarvi graben–syncline to the postorogenic tectono-magmatic activization. The activization favored the formation of contrasting metasomatic associations: magnesian and alkaline (to gumbeitic).

The Maisk deposit is characterized by simple structure and ore mineralogy, but very complicate metasomatic alterations of host rocks. Two stages of metasomatic rock formation are distinguished: an early one, with formation of quartz–biotite–amphibole metaso-

matites and quartz veins, and a later one accompanying the ore deposition.

The formation temperature of the quartz veins and early metasomatites was 470–300°C, and the solutions were heterogeneous, saturated with gas, and of low density and low salinity (1.5–4 wt %). Quartz filled open fractures and replaced host rocks.

The gold and sulfides were deposited at around 200°C from solutions with intermediate salinity (22–26 wt %) that were heterogeneous, consisting of a water–salt solution and a high-density CO_2–CH_4 fluid. The K feldspar metasomatites (gumbeites) probably formed before gold deposition and were accompanied by quartz recrystallization. Sulfides formed under an increase in methane content from 25–16 mol % to 70 mol % and even more, pressure varying from 940 to 500 bar, and temperature varying from 270 to 190°C. The gold was probably deposited at 140–200°C. The recrystallization related to solutions with low gas saturation occurred at 180–110°C. The salt concentration varied in solutions from brines (35–30 wt %) to intermediate values (20–9 wt %).

This data testifies to the two megastages of mineral deposition at the deposit. The inheritance of some mineral assemblages of the second megastage relates to the influence of host rock composition.

According to all of these data, the ore-forming fluids were magmatogenic and enriched with sulfur and ore components probably due to extraction of them from host and more deeply located rocks.

It is difficult to estimate the scale of the gold reserves at the Maisk deposit and in the district using available information. The scanty pocketlike distribution of gold contradicts the mineralogical and geochemical features of ore veins.

The gold-ore assemblages, the structures and textures of the gold-bearing quartz, and the K feldspar–biotite metasomatites at the Maisk deposit are similar to those of the giant Kolar gold deposit (its intermediate levels) in India and at some deposits in the Abitibi belt (Canada).

No signs of significant erosion of the Maisk deposit area are observed. Some shallow boreholes do not give information sufficient to estimate the prospects of extension of ore to a depth. Therefore, the general evaluation criteria suggest a positive outlook regarding quartz gold ores at the Maisk deposit and in the adjacent district.

ACKNOWLEDGMENTS

This study was supported by the federal program "State Support of the Integration of Higher Education and Fundamental Sciences in 1997–2003" and the Russian Foundation for Basic Research, project no. 01-05-64304.

REFERENCES

Brown, P.E., A Fluid Inclusion Data Reduction tion Program, *Second Biennial Pan-Ameri Research on Fluid Inclusions. Prog. with Abst*

Faure, G., *Principles of Isotope Geology*, New 1986. Translated under the title *Osnovy izoto* Moscow: Mir, 1989.

Gaall, G. and Sundblad, K., Metallogeny of G noscandian Shield, *Mineralium Deposita*, pp. 104–114.

Gavrilenko, B.V., Petrashova, L.S., and Dain, zoic Quartz-Vein Gold Deposit Mayskoe in (Russia), *Gold'99 Trondheim (Abstract Volu* 1999, pp. 81–83.

Goldstein, R.N. and Reynolds, T.J., Systema Inclusions in Diagenetic Minerals, *Chort Cou* (Okla): SEPM, 1994.

Lehtonen, M., Manninen, T., Rastas, P., *et al.*, Geologisen Kartan Selirys. Summary and Discu nation to the Geological Map of Central Laplan *Finl., Report of Investigation*, 1985, vol. 71.

Malezhik, V.A., Basalaev, A.A., and Zhanguro Paleogeographical Aspects of Sedimentation Zone of Karelides, *Basseiny sedimentatsii i zon dokembriya Kol'skogo poluostrova* (The S Basins and Precambrian Zones of the Kola Pen tity, 1983, pp. 32–39.

Manttari, I., Lead Isotope Characteristics of Epi Mineralization in the Palaeoproterozoic Laplan Belt, Northern Finland, *Geol. Surv. Finl. E* Bul. 381.

Mints, M.V., Glaznev, V.N., Konilov, A.N., *e dokembrii severo-vostoka Baltiiskogo shchita namika, stroenie i evolyutsiya kontinental'noi* Precambrian of the Northeastern Baltic Shiel Nauchnyi Mir, 1996.

Mitrofanov, F.P., Pozhilenko, V.I., Smolkin, V.F., *ogy of the Kola Peninsula (Baltic Shield)*, Apati

Nickel–Copper Deposits of the Baltic Shield an vian Caledonides, *Geol. Surv. Finl. Espoo*, 1985

Nurmi, P.A., Lestinen, P., and Niskavaara, H., Characteristics of Mesothermal Gold Deposits in candian Shield, and a Comparison with Select and Australian Deposits, *Geol. Surv. Finl. E* Bull. 351.

Ohmoto, H. and Rye, R.O., Isotopes of Sulfur *Geochemistry of Hydrothermal Ore Deposits*, J. Wiley, 1979, pp. 509–567.

Pankka, H. and Vanhanen, E.J., Aulacogen-Re netic Au–Co–U Deposits in Northeastern Finla Research, 1988, *Geol. Surv. Finl. Espoo*, 1989,

Pankka, H.S. and Vanhanen, E., Early Proterozoi Deposits in the Kuusamo Volcano-Sedimentary land, *Precambrian Res.*, 1992, no. 58, pp. 387–4

Rybakov, S.I., Gorodnitskii, L.L., Khazov, R.A., allogenic Epochs and Evolutions of Ore-Formin in the Precambrian of Karelia, *Geol. Rudn.* 1993, vol. 5, no. 5, pp. 371–379.

Sharpe, E.N. and McGeehan, P.J., Bendigo Gold *ogy of the Mineral Deposits of Australia and Guinea*, Parkville, 1990, vol. 2, pp. 1287–1296.

Sundblad, K., Gold Deposits of Fennoscandian Shield, *Gold'99 Trondheim (Abstract Volume)*, Norway, 1999, pp. 51–83.

Turchenko, S.I., Semenov, V.S., Amelin, Ju.V., *et al.*, *The Early Proterozoic Riftogenic Belt of Northern Karelia and Associated Cu–Ni, PGE, and Cu–Au Mineralization*, Stockholm, 1991, vol. 113, part 1, pp. 70–72.

Vaasjoki, M., Lead from Late Archean and Early Proterozoic Mineralization in the Fennoscandian Shield: Constrains on Early Crust-Forming Processes, *Geol. Surv. Finl. Espoo*, 1989, Spec. Pap. 10, pp. 31–33.

Voinov, A.S. and Polekhovskii, Yu.S., The Lower Proterozoic Stratigraphy of Pana–Kuolayarvi Structural Zone (Northern Karelia), *Stratigrafiya nizhnego dokembriya Karelo-Kol'skogo regiona* (The Lower Precambrian Stratigraphy of the Karelia–Kola Region), Leningrad, 1985, pp. 96–106.

Ward, P., Harkonen, I., Nurmi, P.A., and Pankka, H.S., Structural Studies in the Lapland Greenstone Belt, Northern Finland and Their Application to Gold Mineralization: Current Research 1988, *Geol. Surv. Finl. Espoo,* 1989, pp. 71–77.

Zhangurov, A.A., Hydrothermal–Metasomatic Transformations of Metavolcanics in the Kuolajarvi Zone of Karelides, *Metamorfizm i metamorfogennoe rudoobrazovanie rannego dokembriya* (Metamorphism and Metamorphogenic Ore Formation in the Early Precambrian), Apatity, 1984, pp. 25–32.

Zharikov, V.A. and Omel'yanenko, B.I., Classification of Metasomatites, *Metasomatizm i rudoobrazovanie* (Metasomatism and Ore Formation), Moscow: Nauka, 1978, pp. 9–27.